A Raman study of single crystal congruent lithium niobate following electric field repoling.

Jeffrey G Scott*, Sakellaris Mailis, Collin L Sones, Robert W Eason

Optoelectronics Research Centre, University of Southampton,
Highfield, Southampton, SO17 1SY, UK

* = corresponding author
email: jgs@orc.soton.ac.uk
phone: +44 (0)23 8059 4527
fax: +44 (0)23 8059 3142

Abstract

We describe a study of the time dynamics of the spectral position of six major single peaks in the Raman spectrum of single crystal congruent lithium niobate, following the process of electric field repoling. All of the peaks observed show a small ($<1cm^{-1}$) frequency shift after repoling. Two peaks are shifted to higher frequencies while the other four are shifted to lower frequencies. This shift generally recovers over time towards the original value. The $153cm^{-1}$ and $432cm^{-1}$ peaks are seen to recover to their original positions before poling, with time constants of ~ 8 and 4 hours respectively, whereas the higher frequency peak at $872cm^{-1}$ does not appear to recover at all. The other peaks exhibit incomplete recovery. We compare the measured values of temporal recovery to published relaxation times for internal electric fields, and make an additional comparison with our measured etch rate data for the –z face of lithium niobate as a function of delay time following repoling.

Keywords: Raman, lithium niobate, repoling, domain inversion, ferroelectrics.

PACS: 77.84.Dy Niobates, titanates, tantalates, PZT ceramics etc

78.30-HV Raman Spectra – other non-metallic inorganics

77.80.Dj Domain Structure; hysteresis

Introduction

Lithium niobate, $LiNbO_3$, is an important synthetic crystal material due to its unique range of optical and nonlinear optical properties, and has applications in many areas of scientific and technological research and development. Lithium niobate became of considerable interest for use in nonlinear frequency conversion in the past decade, once the technique of high aspect ratio electric field poling (also referred to as domain inversion) had been successfully demonstrated. This technique allows the fabrication of high quality centimetre long samples of periodically poled lithium niobate (PPLN) which has been extensively used to achieve quasi-phase-matched interactions for frequency conversion and optical parametric processes [1,2].

Lithium niobate is in space group R3c and has a distorted perovskite-type structure, below its Curie temperature (1210 °C). Planes of oxygen atoms are arranged in a distorted hexagonal close-packed arrangement, with the interstices alternately filled by lithium atoms, niobium atoms, and vacancies. In a perfect crystal, each Li or Nb atom is surrounded by a distorted octahedron of O^{2-} ions [3]. However, in a real crystal the exact stoichiometry will vary depending on the manufacturing process adopted. The most commonly grown crystal is referred to as congruent and deviates from the ideal stoichiometric $Li_1Nb_1O_3$ composition, showing a small lithium deficiency such that [Li] / ([Li] + [Nb]) = 48.4%.

In the ferroelectric phase the lithium and niobium atoms are displaced from their equilibrium (paraelectric) position, thus defining the direction of the spontaneous polarisation. Poling virgin lithium niobate at room temperature involves applying a large electric field (of order 220 kV cm^{-1}) across the ferroelectric crystal axis (the z-

axis), which displaces both Li and Nb atoms from their equilibrium positions thereby inverting the direction of spontaneous polarisation. For an ideal ferroelectric crystal, this repoling step should produce domain inverted material that is the same in every respect as the virgin crystal, and which has, for example, identical values of coercive field in the 'forward' and 'backward' poling directions. As we further discuss below, this is not the case for lithium niobate and repoling results in a domain reversed material that has several different characteristics compared to the virgin material.

In this paper we present the results of an experimental study of this inequivalence of domain orientation direction using Raman spectroscopy as a diagnostic tool for examining the shift in phonon energies following repoling. Although it might be assumed that the positions of all the lithium niobate constituent atoms can be absolutely specified immediately following a domain inversion process, there is a subsequent longer-term relaxation behaviour associated with the presence of non-stoichiometric point defects and the re-alignment of the associated internal electric fields [4]. This behaviour has been discussed and quantified already by several techniques [5], but the time dynamics associated with movements of individual atoms within a unit cell have not to our knowledge been reported before. It is for this reason that micro-Raman spectroscopy was chosen as it is perhaps the ideal non-destructive precision structural tool for material characterisation with micron-scale spatial resolution.

1.1 - Relaxation effects following repoling.

The hysteresis curve for lithium niobate is asymmetric: an internal field of between ~25 kV cm^{-1} and 50kV cm^{-1} exists in virgin as-grown crystals at room temperature, depending on the sample. This internal field is aligned along the direction of spontaneous polarisation of the virgin material and after electric field repoling, it gradually realigns to the new polarisation direction. The time scale for this process can extend to years, at room temperature. The presence of the internal field has been explained in terms of at least two components of electronic and ionic character [4], which have reported time constants that range from milliseconds to a few seconds, and a few hours to years respectively. The immediate consequence of this internal field is that the coercive fields for forward and reverse poling are not the same. Additionally there is evidence that the etch rate for the –z face of lithium niobate immersed in acid mixtures of HF/HNO_3 is also sensitive to the crystal history subsequent to repoling. Earlier work has investigated the differential etch characteristics between the +z and –z crystal faces and has established that the +z face is effectively immune to etching, even for prolonged exposure at elevated temperatures up to 100°C, while the –z face etches at a rate of ~1μm per hour at room temperature in a 1:2 acid mixture of $HF:HNO_3$ [6].

More recently however, we have observed what we believe to be a related etching behaviour that is a function of the time delay following repoling. Figure 1 shows the measured etch depth of the –z face of four lithium niobate samples cut from a single repoled sample that have been immersed for 20 hours in an acid mixture of $HF:HNO_3$ in a 1:4 volume ratio held at a temperature of 60° C. It is clear from the graph, and the error bars indicated, that for these etch conditions, there appears to be a maximum

etch rate for a time delay of 24 hours following the repoling step. We do not have data for intermediate values of time delay between the first and second measurements, but it would seem apparent that the etching behaviour is sensitive to time delay, and possibly therefore to the presence of internal fields associated with relaxation of the internal crystal structure. Also shown in figure 1 is the etch depth for a time delay of 1000 hours, by which time it appears the crystal structure has undergone some internal relaxation process.

This variation in etch rate is consistent with our previously developed model for the etch chemistry of lithium niobate in HF and HF:HNO_3 acid mixtures [7]. The small relative displacement of the positions of Li and Nb atoms within the unit cell for the two anti-parallel directions of spontaneous polarisation is sufficient to induce an essentially infinite difference in etch rates between the +z and –z crystal faces. The etch rate therefore is a clear indicator of the internal positions of the constituent atoms, so an etch rate that is dependent on time delay following repoling is itself indicative of potentially extremely small differences in atomic positions.

To this end we have employed Raman spectroscopic analysis which is sensitive to any variation in atomic position within a sample, and have observed small (< 1 cm^{-1}) shifts in absolute spectral position and hence frequency of particular vibrational modes and phonon energies, and fitted the measured recovery times to a single exponential recovery process.

1.2 - Raman spectra of lithium niobate.

The primitive unit cell of lithium niobate contains two formula weights (10 atoms), giving 27 degrees of freedom. These are assigned to optical phonon modes with the other 3 as acoustic phonons [8]. Using group theory, the irreducible representations of optical modes of lithium niobate (R3c space group) are found to be [9]:

$$\Gamma_{optical} = 4A_1 + 5A_2 + 9E$$

The E modes are doubly degenerate, thus 27 modes are found, as expected. As only the A_1 and E modes are Raman active, it may be expected to find a total of only 13 phonon peaks. However, long range electrostatic fields in the ionic crystal lifts the degeneracy between longitudinal (LO) and transverse (TO) optical phonons, thereby doubling the number of observed modes [10]. Thus it is possible to detect a total of 26 phonon modes in lithium niobate, by Raman spectroscopy. However, the actual number of peaks that are observed will depend on the relative orientation of the crystal with respect to the spectrometer and the polarisation directions of the incident and scattered light.

2.1 - Experimental procedure.

For purposes of calibration, all spectra recorded for recently repoled samples were referenced to a primary Raman spectrum recorded for a virgin sample of z-cut congruent $LiNbO_3$ taken using a Renishaw Raman microscope, model RM2000. The crystal was then removed from the spectrometer and a small area was repoled, using our standard electric field repoling technique [6]. The sample was then immediately

returned to the Raman microscope for acquisition of repeated scans over periods of several hours.

Small changes in the positions of several of the Raman peaks were readily observed following the repoling step. To ensure however the highest degree of accuracy and consistency for these measurements, and to minimise drift of the Raman spectrometer due to temperature variations within the lab, for example, over the several hours required for the measurements, a neon calibration source was used to provide a reference for each spectrum *during* recording. It was also found that precise and reproducible repositioning of this source was required, as even very small variations of the launch conditions into the Raman microscope would shift the position of the neon peaks by of order one tenth of a wavenumber. A fibre optic launch was therefore implemented to fix the absolute spatial position of light from the neon source. Six neon lines were used with wavelengths (in air) from 6382.99 Å to 6717.04 Å [11], which were converted to the corresponding wavenumber shift with respect to the wavelength of the exciting Helium-Neon laser used which operated at the usual wavelength of 6328.16 Å.

The Raman spectrum was collected using a Z(YY)Z orientation (notation as used in [12]), which corresponds to a 180° back-scattering collection geometry. This configuration gives rise to peaks due to E(TO) and A_1(LO) phonons, and whereas we might expect to observe 13 peaks, only 10 peaks can be readily distinguished. The difference is due to missing E(TO) phonons which are only detected in stoichiometric lithium niobate [13].

A typical Raman spectrum of lithium niobate is shown in figure 2. The sharp lines denoted "Ne" are those from the neon source. The source was switched off whilst the central part of the spectrum was taken, as the neon line at 6506.53 Å spectrally overlapped with the Raman peak at 432cm^{-1}.

The Renishaw Raman spectrometer used in this work had a specified frequency resolution of ~1 cm^{-1}. As noted earlier, without the additional facility of neon calibration, this would have been insufficient to accurately determine the temporal dynamics associated with the relaxation of the Raman peak position following repoling, which typically had values of frequency shift of 1 cm^{-1}. To further increase the measurement precision, all the data from the complete Raman spectrum was separated into parts corresponding to individual peaks, for best-fitting to a Lorentzian profile of the form:

$$y = y_0 + \frac{a}{1+\left(\frac{x-x_0}{b}\right)^2}$$

where a is the height of the peak above y_0 (the baseline) and b is the half-width at half maximum. The peak centre occurs at x_0. A typical example of such a curve-fit is shown in figure 3, for the peak occurring at 581 cm^{-1}. This curve has parameters a = 5304, b = 13.52 cm^{-1}, y_0 = 1331 and x_0 = 580.40 cm^{-1}.

This procedure was applied to the Ne peaks as well as the Raman peaks for lithium niobate, further increasing the precision of the calibration procedures. For each Ne peak, 30 separate measurements and subsequent Lorentzian best fits were performed yielding a final average value of standard deviation of 0.027cm^{-1}. For completeness, table 1 summarises the data set used for the Ne calibration procedure.

2.2 - Experimental results.

The above calibration and best-fit procedures were applied to each of the six representative Raman lines centred at 153, 237, 332, 432, 581 and 872 cm^{-1}, and all subsequent data and analysis of the temporal recoveries relate to these lines only.

Four Raman spectra were taken of a virgin z-cut 300μm thick crystal wafer of lithium niobate, in two different locations on the –z face of the crystal, to establish the precise positions of these six peaks prior to repoling. Domain inversion was then induced in the sample by electric field poling using a voltage of 7.2kV, a current of 500 μA and charge of 39.3 μC. The sample was then returned to the Raman spectrometer, and spectra were taken, approximately every 8 minutes for a total period of 4 hours.

Shown in figure 4 are the results for the Ne-corrected and best-fitted peak positions for these six Raman bands. It is clear in all cases that there is a definite shift in peak position following repoling. Some of the bands (at 153, 237, 581 and 872 cm^{-1}, figs 4(a), (b), (e) and (f)) show a shift to a lower value of wavenumber, whereas the peaks at 332 and 432 cm^{-1} (figs 4(c) and (d)) show a shift in the opposite sense, to a higher value of wavenumber. The peaks at 153, 237 and 432 cm^{-1} experience a subsequent recovery towards their original position, while the 332 and 581 cm^{-1} seem to recover, but not to their original value. The last figure (fig 4(e)) representing the 872cm^{-1} shows the largest shift of ~0.6 cm^{-1}, but no recovery process is apparent over the four hours of measurement. Included in each figure is a dashed line which is the average value of peak position for the four measurements on the virgin material, before repoling.

The solid line in figs 4(a) and 4(d) represents a least squares regression performed to produce an exponential curve fit to the data. A standard exponential decay curve was fitted to the peak at 432 cm^{-1}, while all the 153 cm^{-1} peak was fitted to an exponential rise to maximum curve. The equations used were:

$$\text{Exponential decay: } y = y_0 + ae^{-t/\tau}$$

$$\text{Exponential rise to maximum: } y = y_0 + a(1 - e^{-t/\tau})$$

For the exponential decay curve, y_0 is the average value of peak position before poling and τ is the time constant that corresponds to the time when y (the peak centre) has returned to 1/e of its original value, y_0. The parameters a and τ are determined by the least-squares fitting process.

The exponential rise to maximum curve is similar, but inverted to allow the peak position to increase so that it recovers to the value taken before poling. The y-intercept, y_0, is estimated using a linear extrapolation and the a parameter was chosen so that $(y_0 + a)$, is equal to the mean peak centre value, the maximum in the curve. The least squares regression provides the time constant τ.

The data shown in figures 4(a) and 4(d) is replotted in figures 5(a) and (b), with the exponential curves extrapolated to longer times after poling, to show clearly the recovery process by which these two Raman bands return to their original position following repoling. The time constant for these curves (equivalent to the 1/e recovery time) is 476 minutes for the 153 cm^{-1} peak and 250 minutes for the 432 cm^{-1} peak. Each Raman peak appears to have its own recovery time, with the 432 cm^{-1} band

being the fastest and the 872 cm^{-1} band the slowest, if indeed it does show any recovery process at all. The data from the curves shown in figures 4(a) – 4(f) is summarised in table 2.

3.1 - Discussion

We believe this is the first report of evidence that there is a *dynamic* recovery process that occurs in recently repoled lithium niobate, which can be tracked and measured using the technique of Raman spectroscopy. We have seen one previous report of the use of micro-Raman for such a measurement [14], but this only discloses that there is a shift of several tenths of a wavenumber for a single (unspecified) line, and does not discuss details of any recovery processes for example. The authors in [14] further suggest that the shift observed is likely due to either stress or inequivalence of electric-field poled domains compared to natural poling. No additional details were provided on the time delay between repoling and measuring the small Raman shifts observed.

Perhaps the most interesting point arising from our own measurements concerns the differences in deduced recovery times for the five lines we have studied. It is clear for example that the line at 872cm^{-1} has not recovered during the four hour period of our measurements, while the line at 432cm^{-1} has made a substantial recovery having a 1/e relaxation time of 250 minutes. This is entirely consistent with previous papers that have looked at the multistep electronic and ionic relaxation processes that can occur in both lithium niobate and lithium tantalate, following electric field repoling. Time constants have been observed for the recovery of the internal field for example that vary from 55ms [15], following repoling in the forward direction, through several

days [16], to being incomplete even after a month [4]. Previous authors have used multiple single exponential fits to these processes as well as stretched exponentials [15]. It is clear that the recovery of the internal field is mediated by two, and possibly three, separate relaxation processes, which are of electronic and ionic origins respectively. The longer time constants observed here are consistent with the ionic recovery process as probed by Raman spectroscopy, and themselves show a variation of time constants in the range of several hours and above. Our data is not of sufficiently accuracy in the present study however to attempt anything other than the fitting of a simple single exponential fit.

The etch data presented in figure 1 is further evidence that there is a recovery of the exact atomic (ionic) positions following repoling, which is evident in the factor of two increase in etch rate seen after a time delay of 24 hours. Given the earlier results for etch rates of the +z and –z faces which show an essentially infinite differential etch rate [6], it is therefore to be expected that the very small atomic displacements evident from the < 1 cm^{-1} shifts observed, would translate into a measurable variation of etch rate much less than the differential rate observed between the +z and –z faces. We believe therefore that our measurements that quantify the range of recovery processes that mediate the ionic positions are both consistent with the range of published measurements for recovery of internal electric field, and also extend the physical understanding that underlies the processes involved.

4.1 - Conclusion

In conclusion, we have observed and quantified the shift of frequency of representative bands in the Raman spectrum of lithium niobate immediately following an electric field repoling step. Time constants for two recovery curves have been deduced that fall in the range of several hours and above, and we believe there is consistency between these measurements and those previously published for ionic recovery processes whose time constants are in the hours to days region (and above).

Acknowledgements.

We are pleased to acknowledge Fabrice Birembaut, Mark Bradley, Bill Brocklesby and Jeremy Frey from the Department of Chemistry and the Optoelectronics Research Centre for use of the micro-Raman spectrometer. We would like to thank Professor Marc Fontana of Supélec, Stephen Smith of the University of Essex and Perry Yaney of the University of Dayton for the helpful discussions on this subject. We are also happy to acknowledge financial support from the Engineering and Physical Sciences Research Council (EPSRC) for research funding.

References

[1] M. Yamada, N. Nada, M. Saitoh, K. Watanabe: Appl. Phys. Letts. **62**, 435, (1993)

[2] L.E. Myers, R.C. Eckardt, M.M. Fejer, R.L. Byer, W.R. Bosenberg, J.W. Pierce: JOSA-B **12**, 2102, (1995)

[3] R. S. Weis, T. K. Gaylord: Appl. Phys. A **32**, 191 (1985).

[4] V. Gopalan, T. E. Mitchell: J. Appl. Phys. **83**, 941 (1998).

[5] V.Gopalan, T.E.Mitchell, Y.Furukawa, K.Kitamura: Appl. Phys. Letts., **72**, 1981, (1998)

[6] I.E.Barry, G.W.Ross, P.G.R.Smith, R.W.Eason, G.Cook: Mater. Lett. **37**, 246, (1998)

[7] C.L.Sones, S.Mailis, W.S.Brocklesby, R.W.Eason, J.R.Owen: J. Mater. Chem. **12**, 295, (2002)

[8] C. Kittel: Introduction to Solid State Physics (John Wiley and Sons Inc., New York, 1996).

[9] Y. Repelin, E. Husson, F. Bennani, C. Proust: J. Phys. Chem. Solids **60**, 819 (1999).

[10] W. D. Johnston, I. P. Kaminow: Phys. Rev. **168**, 1045 (1968).

[11] D. R. Lide: CRC Handbook of Chemistry and Physics, 75th Edition (CRC Press, Boca Raton, 1994)

[12] T. C. Damen, S. P. S. Porto, and B. Tell: Phys. Rev. **142**, 570 (1966).

[13] A. Ridah, P. Bourson, M. D. Fontana, G. Malovichko: J. Phys.: Condens. Matter **9**, 9687 (1997).

[14] E.Laubacher, Y. Guan, P. Yaney: Abstract for the OSS00 Meeting of the American Physical Society, Ohio Section Spring Meeting, May 2000 University of Cincinnati, Cincinnati, Ohio USA.

[15] J. H. Ro, M. Cha: Appl Phys Letts, **77**, 2391, (2000)

[16] V.Gopalan, M.C.Gupta: Ferroelectrics, **198**, 49, (1997)

Figure Captions

Figure 1. Measured etch depth for the –z face of recently repoled samples of lithium niobate as a function of delay time between repoling and etching.

Figure 2. A typical $LiNbO_3$ Raman spectrum, with neon reference lines.

Figure 3. Example of Lorentzian fit to the Raman data.

Figure 4. Measured positions of the peaks for the five Raman lines used, as a function of time delay following repoling. Dashed lines represent the peak position for virgin material.

a) 153 cm^{-1} Raman Peak
b) 237 cm^{-1} Raman Peak
c) 332 cm^{-1} Raman Peak
d) 432 cm^{-1} Raman Peak
e) 581 cm^{-1} Raman Peak
f) 872 cm^{-1} Raman Peak

Figure 5. Exponential fits to the Raman lines at 153cm^{-1} and 432cm^{-1} showing time constant for recovery.

a) 153 cm^{-1} Raman Peak
b) 432 cm^{-1} Raman Peak

Table 1. Neon emission line data and measured spectral standard deviation for three lines.

Table 2. Summary of results and parameters from fitting of exponential curves to the data.

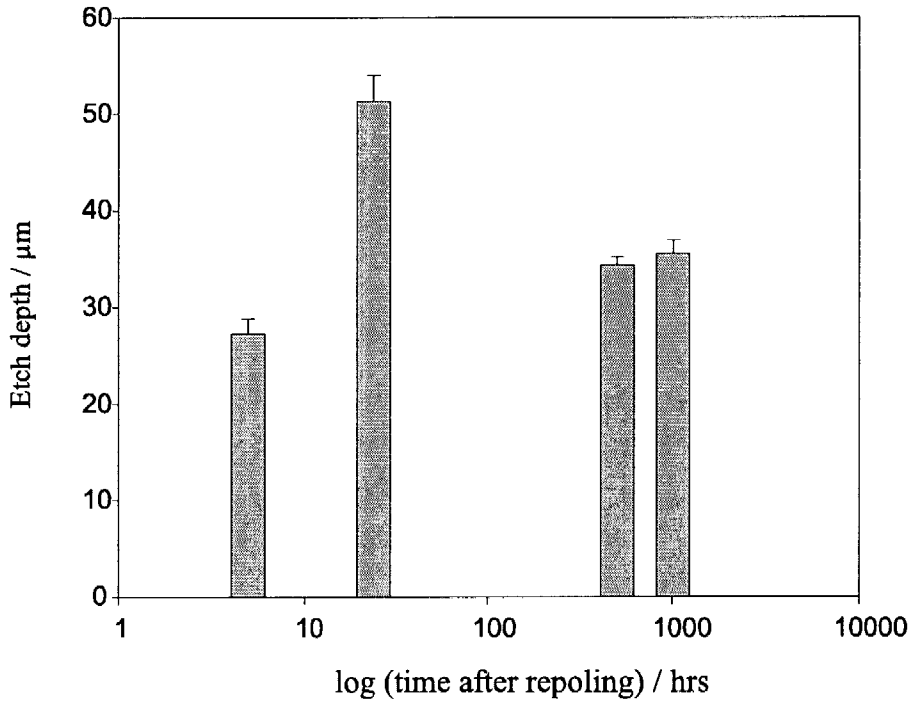
60
50
40
30
20
10
0
Etch depth / µm
1
10
100
1000
10000
log (time after repoling) / hrs

Figure 1.

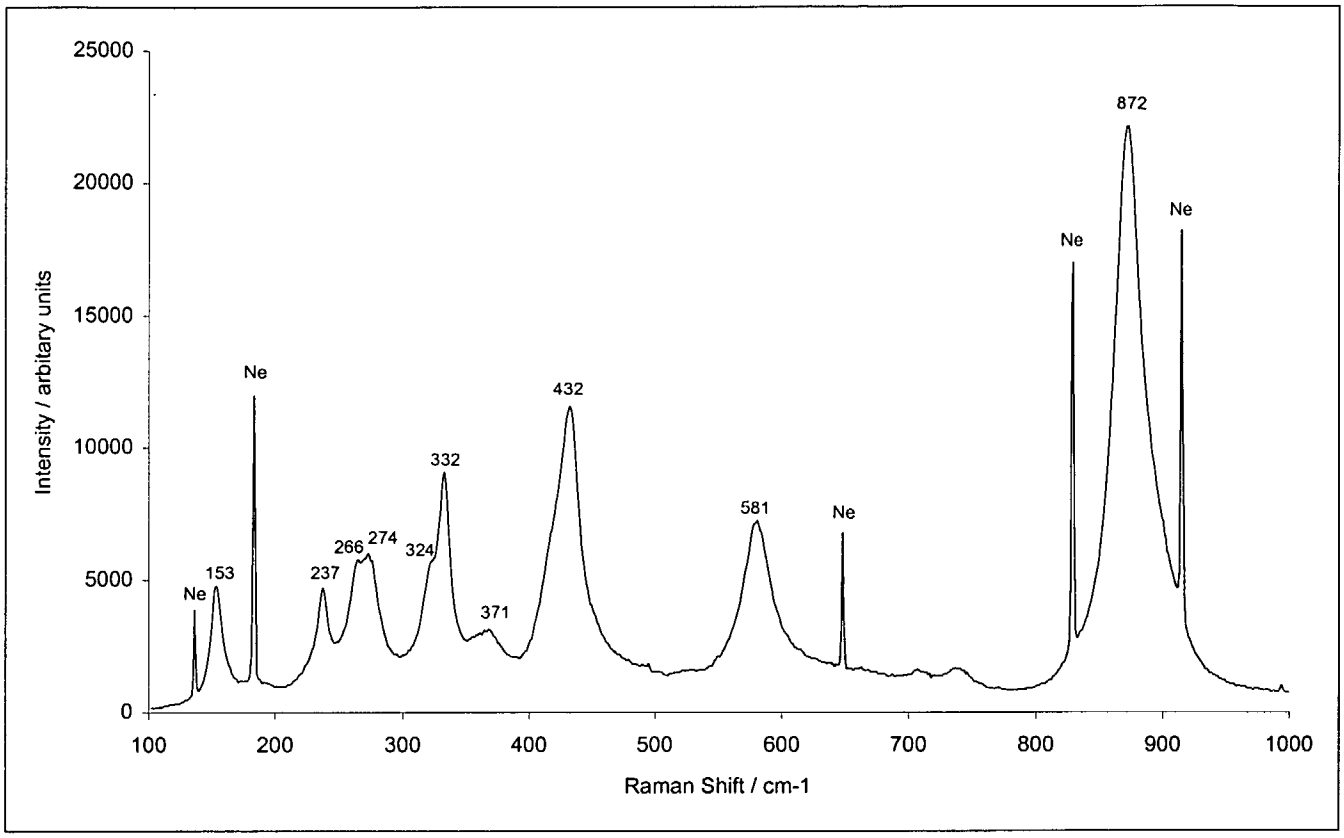
25000
20000
15000
10000
5000
0
Intensity / arbitary units
100
200
300
400
500
600
700
800
900
1000
Raman Shift / cm-1
Ne
153
Ne
237
266
274
324
332
371
432
581
Ne
Ne
872
Ne

Figure 2

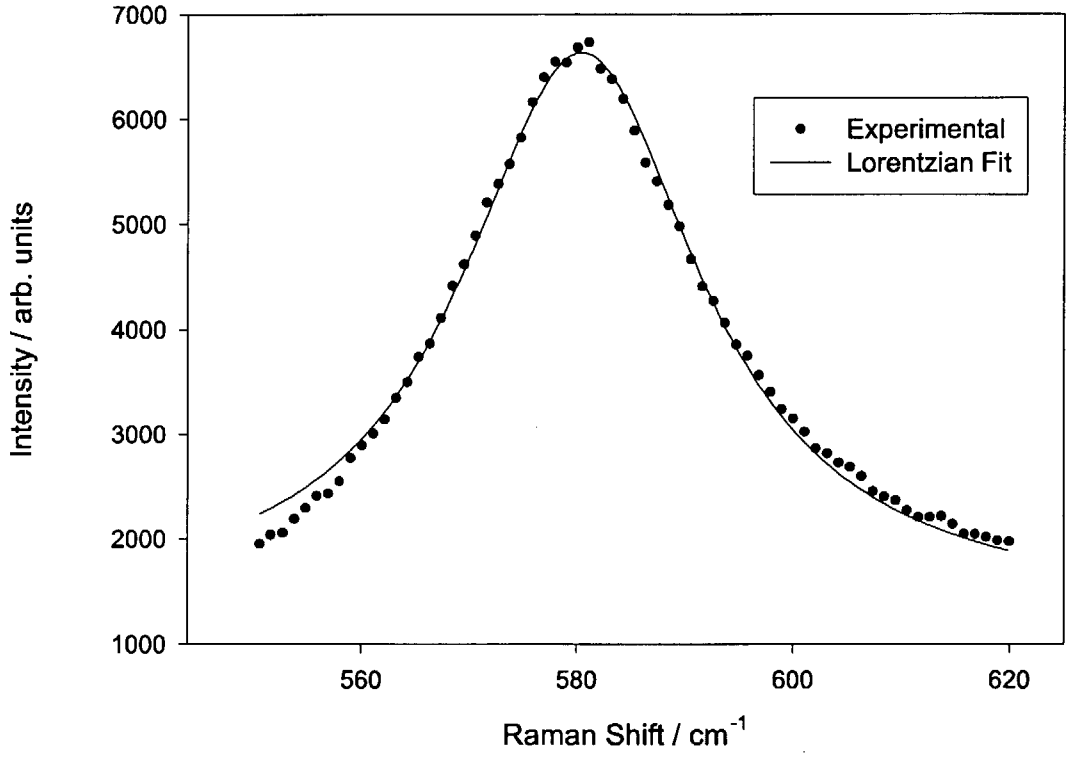
7000
6000
5000
4000
3000
2000
1000
Intensity / arb. units
560
580
600
620
Raman Shift / cm-1
Experimental
Lorentzian Fit

Figure 3

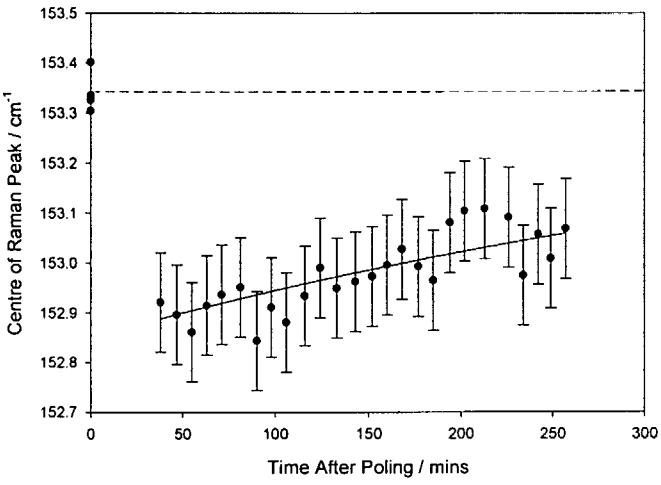

a) 153 cm^{-1} Raman Peak

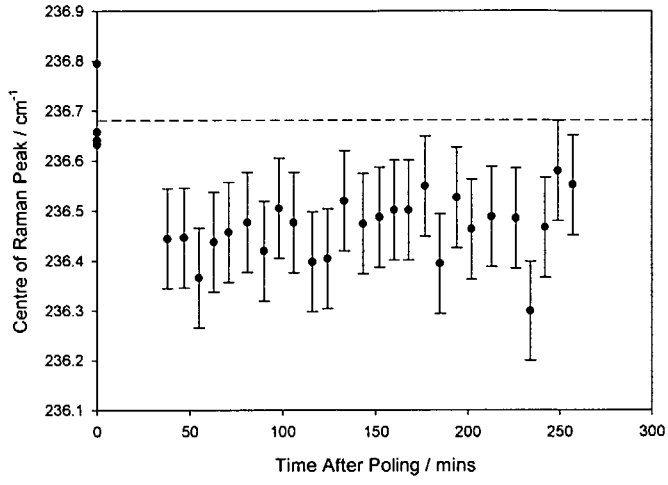

b) 237 cm^{-1} Raman Peak

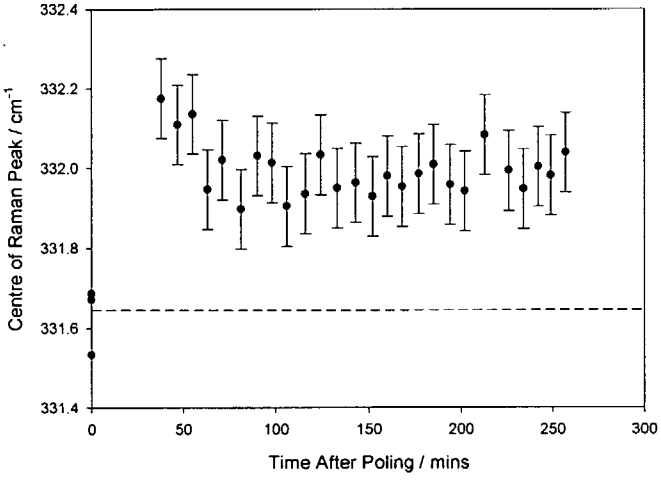

c) 332 cm^{-1} Raman Peak

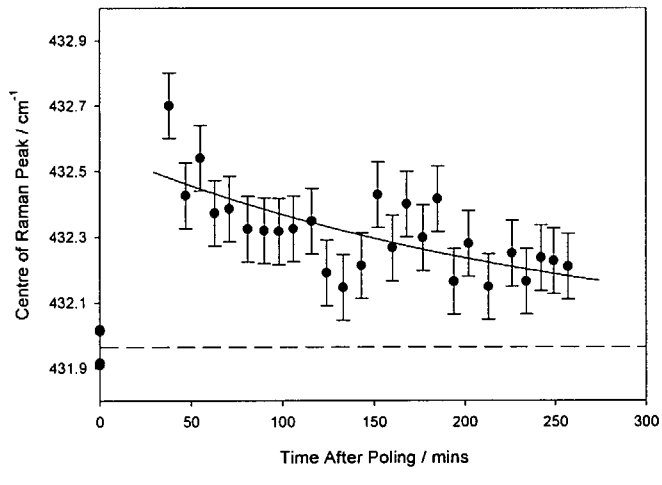

d) 432 cm^{-1} Raman Peak

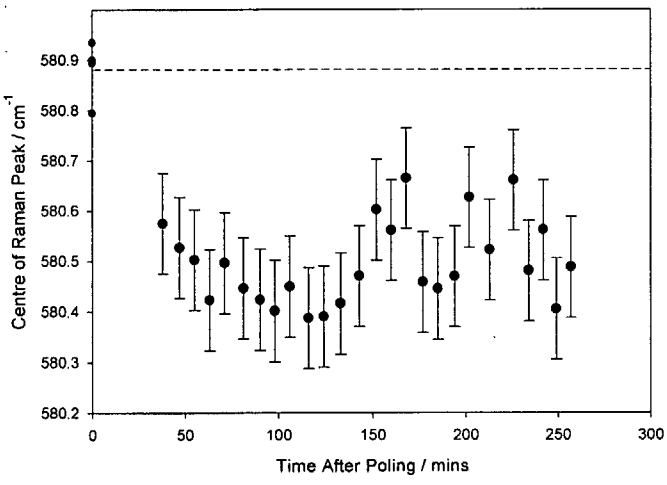

e) 581 cm^{-1} Raman Peak

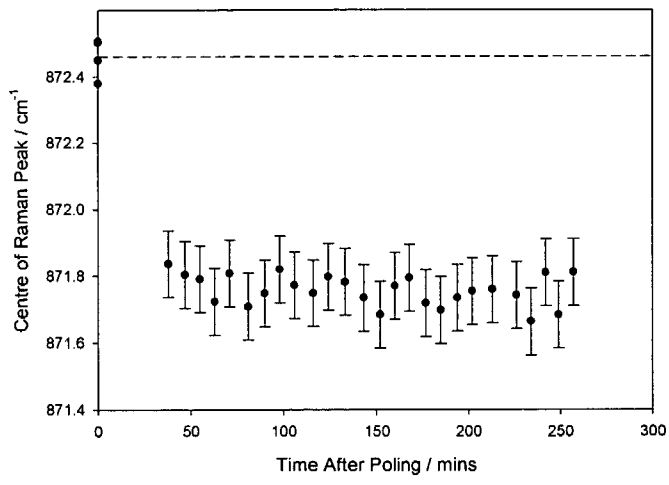

f) 872 cm^{-1} Raman Peak

Figure 4

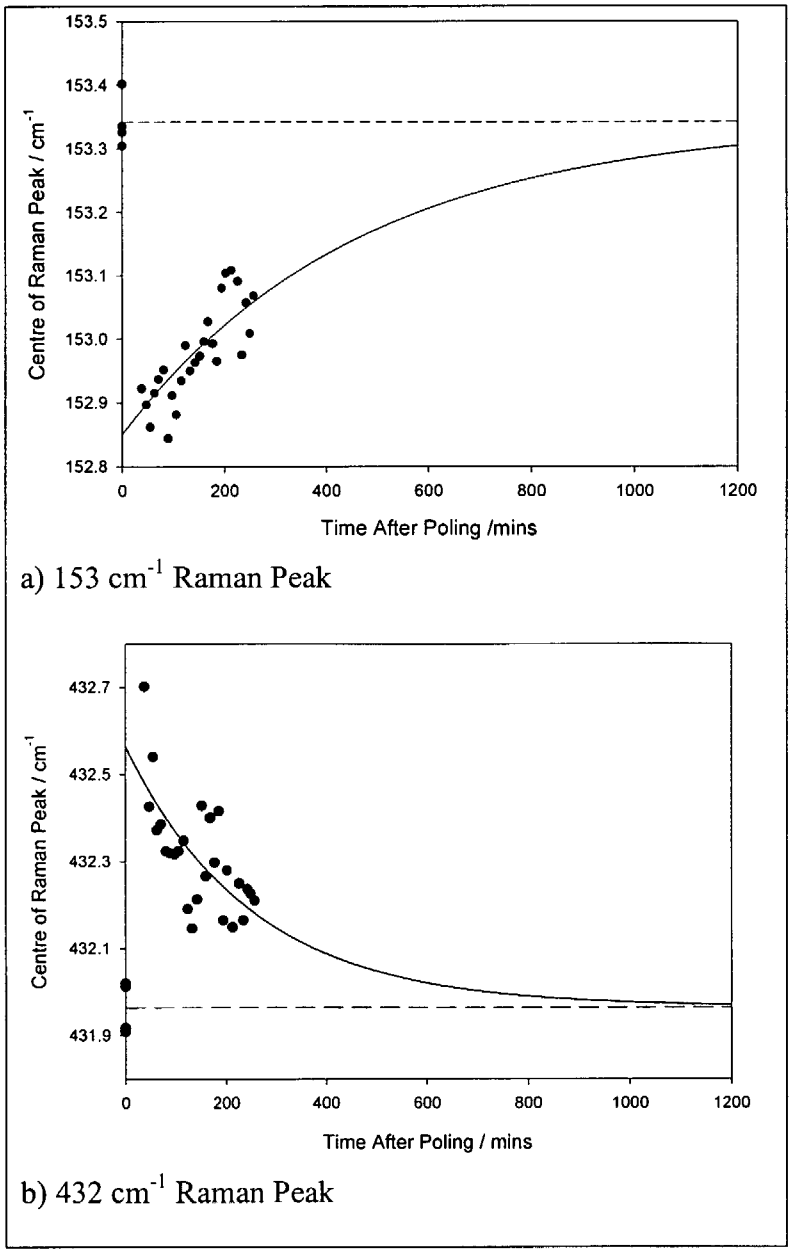

Figure 5

Wavelength / Å (in air)	Absolute Frequency / cm^{-1}	Wavenumber shift relative to He-Ne laser line / cm^{-1}	Standard deviation for 30 measurements / cm^{-1}
6382.992	15666.634	135.734	-
6402.246*	15619.519	182.850	0.028
6598.953*	15153.919	648.449	0.032
6678.276*	14973.924	828.444	0.022
6717.043	14887.503	914.865	-

* = used for calibration of Raman lines

Table 1

Raman Peak (cm^{-1})	Peak Centre before poling (cm^{-1})	Peak Centre after poling (cm^{-1})	Difference (cm^{-1})	% Change	y_0 (cm^{-1})	A (cm^{-1})	τ (mins)
153	153.34	152.90	-0.44	-0.29	152.85	0.492	476
237	236.68	236.42	-0.26	-0.11	-	-	-
332	331.65	332.09	0.45	0.13	-	-	-
432	431.96	432.51	0.55	0.13	431.964	0.5994	250
581	580.88	580.51	-0.37	-0.06	-	-	-
872	872.46	871.79	-0.67	-0.08	-	-	-

Table 2